

A theoretical study on nitric oxide reductase activity in a ba_3 -type heme-copper oxidase

L. Mattias Blomberg*, Margareta R.A. Blomberg, Per E.M. Siegbahn

Department of Physics, Stockholm University, SE-106 91 Stockholm, Sweden

Received 12 July 2005; received in revised form 7 October 2005; accepted 2 November 2005

Available online 7 December 2005

Abstract

The mechanism of nitric oxide reduction in a ba_3 -type heme-copper oxidase has been investigated using density functional theory (B3LYP). Four possible mechanisms have been studied and free energy surfaces for the whole catalytic cycle including proton and electron transfers have been constructed by comparison to experimental data. The first nitric oxide coordinates to heme a_3 and is partly reduced having some nitroxyl anion character ($^3\text{NO}^-$), and it is thus activated toward the attack by the second NO. In this reaction step a cyclic hyponitrous acid anhydride intermediate with the two oxygens coordinating to Cu_B is formed. The cyclic hyponitrous acid anhydride is quite stable in a local minimum with high barriers for both the backward and forward reactions and should thus be observable experimentally. To break the N–O bond and form nitrous oxide, the hyponitrous acid anhydride must be protonated, the latter appearing to be an endergonic process. The endergonicity of the proton transfer makes the barrier of breaking the N–O bond directly after the protonation too high. It is suggested that an electron should enter the catalytic cycle at this stage in order to break the N–O bond and form N_2O at a feasible rate. The cleavage of the N–O bond is the rate limiting step in the reaction mechanism and it has a barrier of 17.3 kcal/mol, close to the experimental value of 19.5 kcal/mol. The overall exergonicity is fitted to experimental data and is 45.6 kcal/mol.

© 2005 Elsevier B.V. All rights reserved.

Keywords: Nitric oxide reductase; NOR; Heme-copper oxidase; Cytochrome *c* oxidase; CuO ; Reduction; Electron transfer; Nitrous oxide; Nitric oxide; DFT; B3LYP

1. Introduction

The ba_3 heme-copper oxidase is a membrane bound terminal enzyme in the respiratory chain of the prokaryote *Thermus thermophilus*. The enzyme belongs to the heme-copper oxidase family and catalyzes the reduction of dioxygen to water in a four-electron reduction, while oxidizing cytochrome c_{552} . Dioxygen is used as the electron acceptor and the exergonic reduction is coupled to the translocation of protons across the inner cell membrane of the bacteria. The redox energy is converted into an electro-chemical gradient, which drives the synthesis of ATP.

Cytochrome oxidases and nitric oxide reductase (NOR) both belong to the heme-copper oxidase family and may have developed from a common ancestor. The catalytic subunit in NOR, NorB, corresponds to subunit I in cytochrome oxidases

and their tertiary structures are believed to be very similar [1]. Nitric oxide reductase and cytochrome oxidase have significant sequence homology with all six metal binding histidines conserved. Both types of enzymes have a binuclear active site consisting of a heme and Cu_B in cytochrome oxidase, whereas Cu_B is exchanged for Fe_B in NOR [2,3]. Nitric oxide reductase catalyzes the two-electron reduction of two nitric oxides to nitrous oxide and water.

Discovering the structural similarities between cytochrome *c* oxidases and NOR raised the question whether cytochrome *c* oxidase can catalyze the reduction of nitric oxide, and vice versa if NOR can catalyze the reduction of O_2 . The inhibition of cytochrome oxidases by NO have been known for a long time and recently several cytochrome oxidases have also been shown to display nitric oxide reductase activity, supporting the hypothesis of the two types of enzymes having a common phylogeny. The two cytochrome oxidases of *Thermus thermophilus*, ba_3 [4] and caa_3 [4] both reduce NO. Furthermore the cytochrome cbb_3 from *Pseudomonas stutzeri* [5] and the cytochrome bo_3 from *Escherichia coli* [6] have been shown to

* Corresponding author.

E-mail address: mattiasb@physto.se (L.M. Blomberg).

display NOR activity, while bovine cytochrome *c* oxidase does not. The bacterial NOR *Paracoccus denitrificans* ATCC 35512 is the only nitric oxide reductase to date which has been shown to be able to reduce O_2 [7].

In the last 10 years, the structures of several cytochrome oxidases have been determined of which the ba_3 -type oxidase of *Thermus thermophilus* and bo_3 -type oxidase of *Escherichia coli* have been shown to reduce NO. In contrast, no structure has to date been determined for a respiratory nitric oxide reductase.

The scarcity of structural information of NOR has turned some of the focus to the NO reduction in different types of cytochrome oxidases. The mechanism with which NO is reduced in cytochrome oxidases may be similar to the one in nitric oxide reductase. Furthermore, since NOR is believed not to pump protons, the difference between the two enzymes may also reveal information about the proton translocation mechanism.

In the present study, the mechanism of the nitric oxide reductase activity in the ba_3 -type oxidase of *Thermus thermophilus* has been studied using density functional theory (B3LYP). A reaction mechanism for the reduction of NO in the ba_3 -oxidase is proposed and the order of the incoming protons and electrons during the catalytic cycle is discussed.

2. Model

The ba_3 -oxidase is the terminal oxidase showing the highest NOR activity of those for which an X-ray structure has been determined [8], see Fig. 1 for the structure of the binuclear center with surroundings. In the present study, the fully reduced active site of the ba_3 -oxidase have been used as the starting point in the calculations. In the cytochrome

oxidases, displaying NO reductase activity the fully reduced enzyme is the active form (ba_3 , caa_3 , bo_3) except in the cbb_3 -oxidase where heme b_3 is believed to have a relatively low redox potential which thus is not so easily reduced [5]. However, since all the redox active metal sites, except heme b_3 , are reduced an electron can be rapidly delivered when NO binds.

The active site (a_3 -Cu_B) in the ba_3 -type of oxidase is very similar to the bovine one. Cu_B is coordinated to three histidines, His282, His283 and His233, where His233 is covalently bonded to Tyr237. Heme a_3 is coordinated to His384 and propionate A is hydrogen bonding to His376 and Asp372. Propionate D forms a salt bridge to Arg449.

In the present study, two models of the active site binuclear center have been used. The final energies are taken from the larger model, while the smaller one, for which the Hessians could be calculated, was used in the localization of the transition states. The large model consists of around 108 atoms which made the frequency calculations too time consuming.

The heme group is modeled as a porphyrin ring without substituents. In the smaller model, all histidines are modeled as imidazoles where the C_β of the histidines are substituted for hydrogens which are frozen at a typical imidazole C–H bond length along the C_γ–C_β bond in the crystal structure. In the extended model, the proximal His384 is modeled as a 4-ethylimidazole with the C_α of the histidine frozen. His233–Tyr237 is modeled as a 1-methyl-4-ethyl-imidazole with the C_α and the Tyr237 meta-carbon frozen. The Tyr237 residue is assumed not to be crucial for the reduction of NO and therefore the Tyr237 ring is not included in the model of the binuclear center. The two adjacent His282 and His283 and the backbone connecting them are incorporated into the model with the peptide nitrogen frozen. All frozen coordinates in the

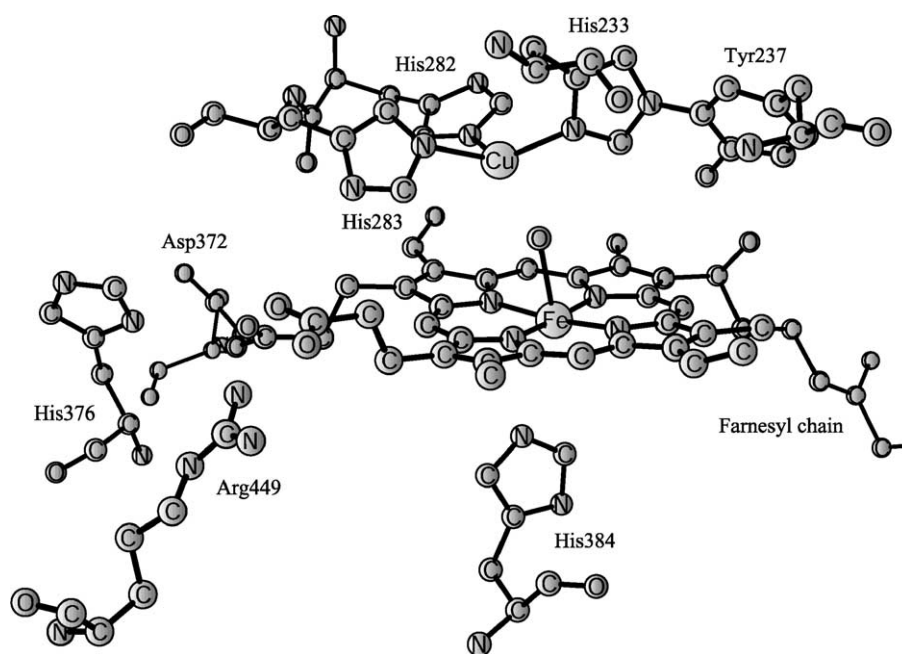


Fig. 1. The crystal structure of the binuclear active site of the ba_3 -type of oxidase in *T. thermophilus*.

extended model are taken from the crystal structure. Furthermore, a model incorporating only the heme side of the binuclear center, excluding Cu_B with its histidine ligands, was used to calculate the bond strength between the ferric heme and N_2O .

Both models used in the calculations have restrictions according to the crystal structure. The smaller model turned out to be too constrained for some of the intermediates during the catalytic cycle, giving errors in the relative energies. Therefore it was not possible to optimize all transition states with this model. In the cases where the transition states could not be optimized, they were localized by scanning one or two bond distances using the larger model.

3. Methods

The geometries of the stationary points involved in the reaction studied were optimized using Becke's [9] three parameter hybrid exchange functional combined with the Lee-Yang-Parr [10] correlation functional (B3LYP). The calculations were performed using the GAUSSIAN-03 [11] and JAGUAR [12] programs. The geometries were optimized with the double- ζ quality basis set lacvp implemented in JAGUAR [12] with an effective core potential (ECP) on iron and copper. Most intermediates are open shell systems, which were treated using unrestricted B3LYP.

The models used in the present study have coordinates frozen according to the X-ray structure and thus entropy corrections from the vibrational frequencies cannot be used. The entropy effect is estimated to be 10 kcal/mol when a di- or tri-atomic molecule is bound or released [13,14]. Furthermore, it has been shown for similar reactions that the entropy cost in the transition state when binding di- and triatomic molecules is around 1 kcal/mol less compared to the entropy cost of forming the bond [13,14]. Because the entropy correction is not calculated, the same entropy correction is used for both transition and bound states. The relative energies discussed below are Gibb's free energies in solution.

The final energies for the optimized geometries were evaluated using the lacvp3p**+basis set of JAGUAR, which is a triple-zeta basis set with an ECP on the metal ions and including one diffuse function on all heavy atoms and one polarization function on first and second row atoms. The dielectric effects from the surrounding environment were obtained for all stationary points using the Jaguar self-consistent reaction field method [15] using the lacvp basis set. The dielectric constant was set equal to 4 [16]. The probe radius of the solvent was set to 1.4 Å, which corresponds to the radius of a water molecule.

Describing the surrounding protein matrix as a dielectric continuum is a rather crude model especially when calculating electron and proton affinities. The importance of the description of the charges and inhomogeneity of the protein on pK_a values in cytochrome *c* oxidase has been emphasized [17]. In that case the position of the protonation is located at the surface of the quantum chemical model and the interactions with the surrounding are thus only described by the dielectric medium and protein charges, which then are crucial for tuning the pK_a values. However, in the present study, the positions of the protonation of different intermediates are located in between the two metal ions and the most important interactions are thus described by the quantum chemical model. Furthermore, the total charge of the model is the same for all calculated electron (+2) and proton affinities (+1), respectively. By comparing intermediates where the total charge is equal and the most important interactions are described by the quantum chemical model, the effects of the surrounding protein should be very similar.

The accuracy of the B3LYP functional has been tested in the extended G3 benchmark set [18], which consists of enthalpies of formation, ionization potentials, electron affinities and proton affinities for molecules containing first- and second-row atoms. The B3LYP functional gives an average error of 4.3 kcal/mol [18] for 376 different entries. Due to the lack of accurate experimental data for transition metals there are few extended benchmark tests. Normal metal–ligand bond strengths indicate that the errors can be slightly larger, 3–5 kcal/mol

[19]. Different aspects of modeling enzyme active sites have been reviewed [20,21].

4. Results and discussion

In the present section, the different reaction steps in the reduction of nitric oxide to nitrous oxide in a ba_3 -type cytochrome oxidase are discussed. The overall reaction is given in Eq. (1). In the formation of N_2O and H_2O an N–N bond is formed and an N–O bond is broken, while two electrons and two protons are transferred to the binuclear center.



The two electrons reducing the two NO's can primarily be supplied through oxidation of the binuclear center, which at a later stage can be reduced by electrons coming from a reductant (cytochrome c_{552}), via Cu_A and heme *b*, regenerating the fully reduced active site. An important and difficult problem is to determine exactly at which points the electrons and protons enter the active site during a catalytic cycle. One way of determining this issue is to calculate the electron affinity (EA) of the different intermediates. The EA obtained can then be compared to the cost of oxidizing the electron donor, in this case heme *b*. Unfortunately, the energetics of the electron transfers are difficult to estimate since electron affinities are sensitive to the surroundings, and thus to the model used. However, relative values within the same model are generally much more accurate, as discussed in Section 3. The energetics of the proton transfers have similar difficulties since the source of the protons is not known, and also the proton affinities are sensitive to the surroundings.

Four mechanisms have been investigated for the reduction of NO in a ba_3 -type cytochrome oxidase. Two of the mechanisms (A and B) go via a hyponitrite intermediate and differ mainly in the order of the rate limiting breakage of the N–O bond and the first electron transfer from heme *b*. Case A and B are discussed in detail in Sections 4.1–4.5. In the other two cases (C and D) an isomer of hyponitrous acid is formed and thus a second proton is needed before the N–O bond can be broken forming N_2O and H_2O . The cases C and D are summarized in Sections 4.6 and 4.7. An overview of the investigated mechanisms is given in Fig. 2, where the mechanism marked by the gray area is case B. The latter was found to be the most favored reaction mechanism in the present study. In Sections 4.1 and 4.2, the calculated energies for the reaction steps of cases A and B are presented including transition states for the bond forming and bond cleaving steps. The energetics for the proton and electron transfers, obtained by comparison to experimental data, are considered below in Section 4.3 yielding energy profiles for the entire catalytic cycles discussed in Sections 4.4–4.7.

4.1. Case A

In case A, the protons and electrons entering during the catalytic cycle are incorporated into the model at stages where they are needed for the reaction to be able to proceed.

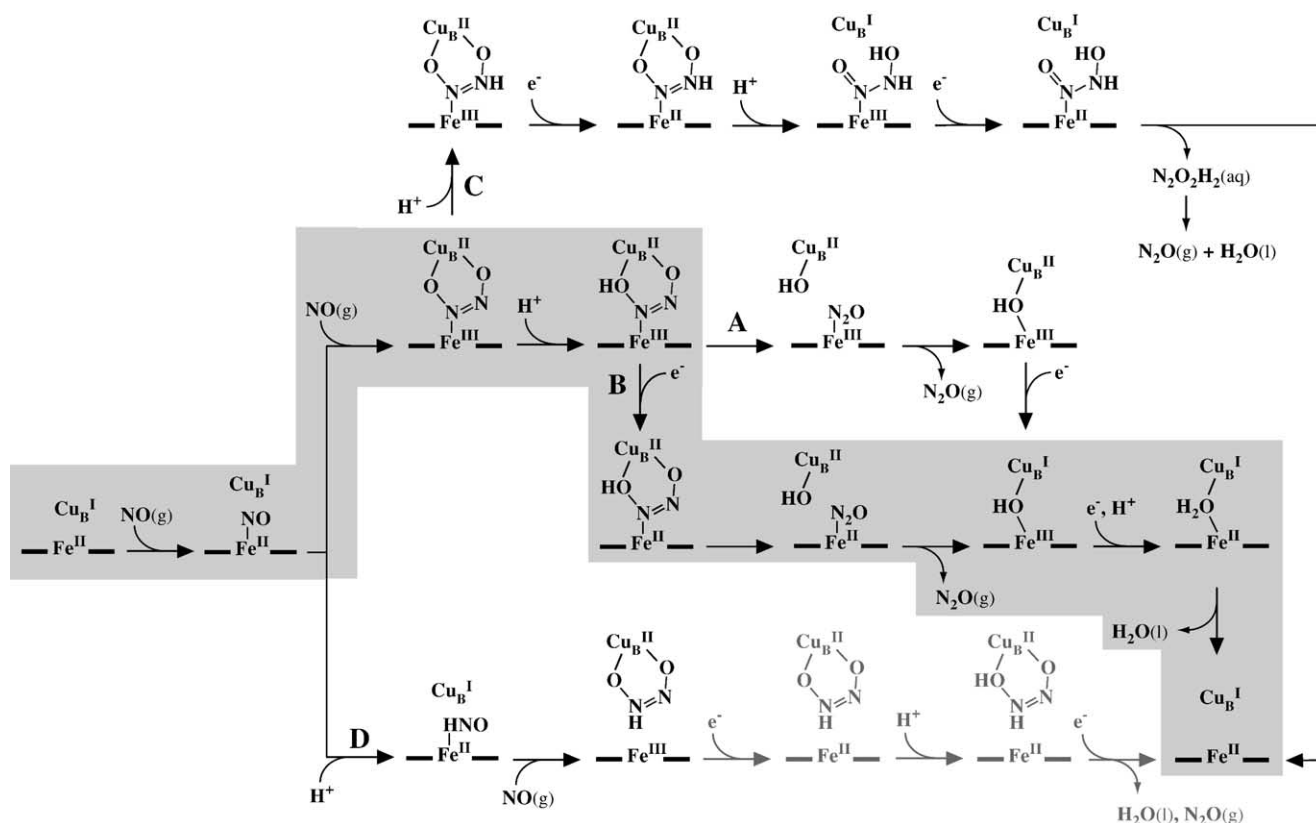


Fig. 2. An overview of the reaction mechanisms investigated for the NO reduction. Case B is marked with a gray area and is the most favored mechanism, see Sections 4.2 and 4.5. The part of case D which is gray has not been investigated in the present study.

4.1.1. Binding of nitric oxide to the binuclear center

Several different coordinations of NO in the binuclear site has been tested showing that NO clearly prefers to bind with its nitrogen to the ferrous heme iron as expected regarding NO's high affinity for Fe(II) complexes [22]. The free energy of binding of NO to Fe(II) is -0.3 kcal/mol. Binding a second NO to the binuclear center appeared to be endergonic. Thus it can be concluded that only one of the NO's is bound in the active site with the nitrogen coordinating to the heme iron. This result fits well with experimental findings where the binuclear center of the *ba*₃-oxidase has been found to bind one equivalent of nitric oxide/enzyme [4]. Furthermore, flash photolysis experiment [23] on NO in cytochrome *c* oxidase imply that the Cu_B–NO bond is weak in agreement with the calculations.

In a previous study, the bond strength between the heme iron and diatomic molecules, and particularly the bond strength of NO, were shown to be underestimated using the B3LYP functional [24]. The latter can give minor errors in the relative energies but these should not affect the conclusions made in the present study.

Binding the first NO to the fully reduced binuclear center partly oxidizes the heme iron to a state in between low spin Fe(II) and Fe(III) with a spin population of 0.30. Nitric oxide has a spin population of -0.75 on N1 and -0.46 on O2, showing that it has some nitroxyl anion character ($^3\text{NO}^-$), the latter has the same electronic configuration as $^3\text{O}_2$. Cu_B stays

closed shell Cu(I), see Fig. 3 for distances and spin populations.

4.1.2. Forming the N–N bond

Experimentally the nitroxyl anion ($^3\text{NO}^-$) is known to react very fast with nitric oxide in solution [25], whereas two nitric oxide molecules cannot form a stable covalent bond. Thus, NO coordinated to the binuclear center should be activated toward the attack from the second NO by the partial reduction.

The potential energy surface for the formation of the N–N bond between the two nitric oxides is very flat and therefore it was not possible to optimize the transition state. However, there should be an entropy barrier in the formation of the bond and the approximate transition state seen in Fig. 4 was found by scanning the N1–N2 bond distance. Adding the effects of the solvation and big basis set the enthalpy barrier of the approximate transition state is 4.0 kcal/mol with respect to one free NO and one coordinated to the binuclear center. Adding the assumed entropy cost of forming the transition state structure of 10.0 kcal/mol gives a Gibbs's free energy barrier of 14.0 kcal/mol.

In the transition state, the spin population on the heme iron has increased slightly from 0.30, when one NO is coordinated to the heme iron, to 0.44. The two nitrogens have opposite spins with a spin population of -0.64 on the nitrogen coordinated to the heme (N1) and 0.51 on the second NO's

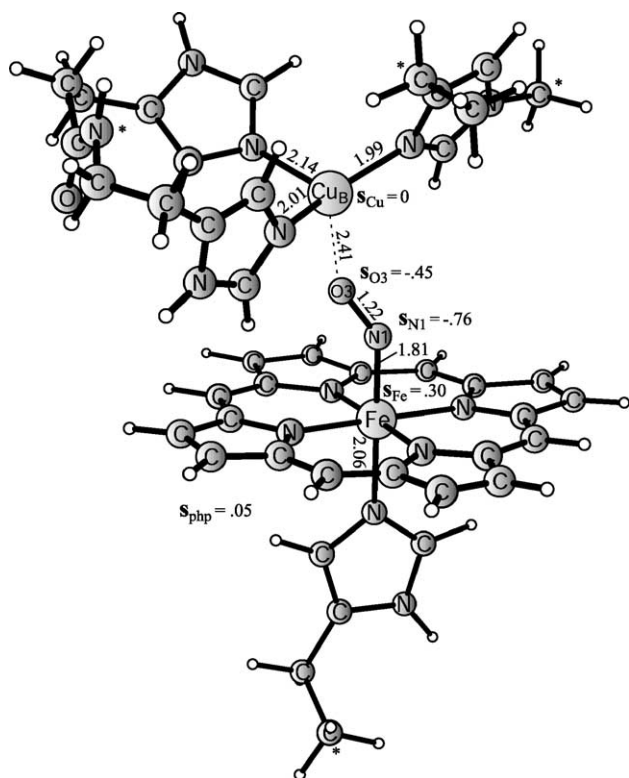


Fig. 3. The binding of one nitric oxide in the fully reduced binuclear center.

nitrogen (N2). The oxygen coordinated to Cu_B (O3) and the oxygen (O4) of the second NO have spin populations -0.41 and 0.19 , respectively. The spin populations imply that there is

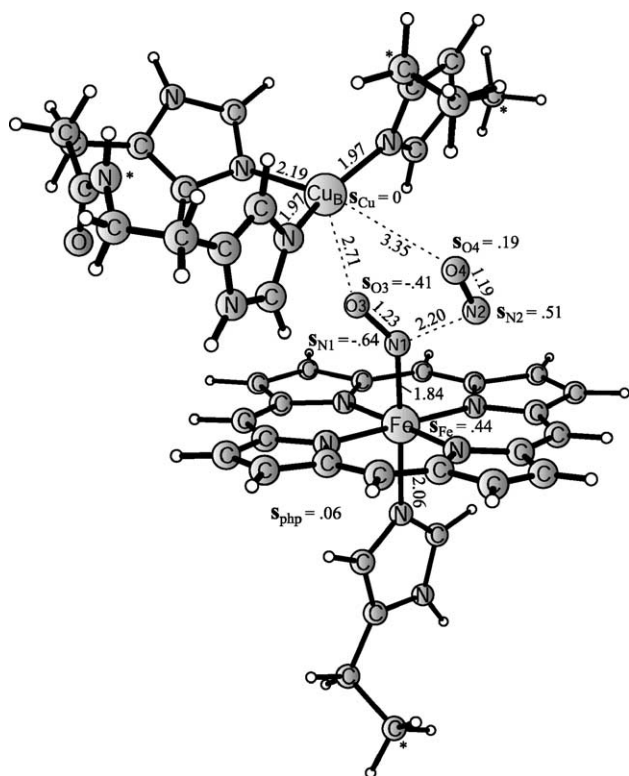


Fig. 4. The transition state of the N1–N2 bond formation (TS1).

transfer of spin density from the $\text{Fe(II)}\text{--NO}$ moiety to the second NO at the transition state, see Fig. 4 for distances and spin populations. After the formation of the N–N bond both oxygens coordinate to Cu_B forming a five-membered ring, see Fig. 5. This structure corresponds to an isomer of hyponitrous acid with the protons replaced by the metal ions, stabilizing the structure in a similar way. The heme iron has now a spin population of 1.05 and is thus fully oxidized to Fe(III) . Cu_B is oxidized to Cu(II) and has a spin population of -0.58 , a typical spin population of a Cu(II) complex. The $\text{N}_2\text{O}_2^{2-}$ (hyponitrous acid anhydride) formed has been reduced by two electrons and the two negative oxygens are stabilized by Cu_B (II). Quite interesting to note is the immediate formation of a double bond between the two nitrogens creating a large driving force for this reaction step. As discussed above, the binding energy of NO to the binuclear center is underestimated by $7\text{--}8$ kcal/mol. The transition state (TS1) in which the five-membered ring is formed is very early, see Fig. 4, which implies that the bond strength of NO to the binuclear center in the transition state should be underestimated by approximately the same amount as the NO bound in the fully reduced case. The barrier height of TS1 should thus not be affected by the underestimated bond strength.

The spin population on the nitrogens and oxygens in the five-membered ring is low, see Fig. 5 for spins and distances, and the reaction is exergonic by 11.7 kcal/mol relative to the NO coordinated to the binuclear center and a free NO. The formation of the cyclic $\text{N}_2\text{O}_2\text{--Cu}_B$ structure is thus quite

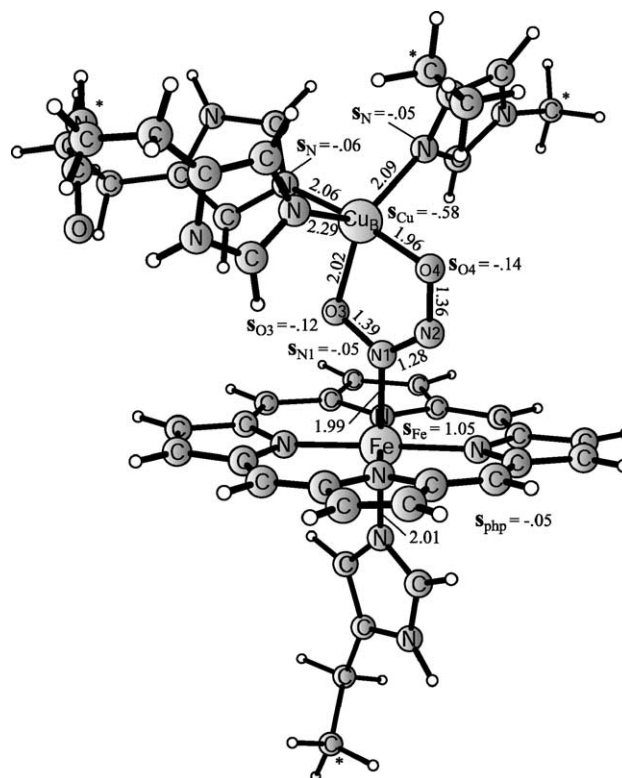


Fig. 5. The five-membered ring with N1 coordinating to the heme Fe(III) and O3 and O4 coordinating to $\text{Cu}_B(\text{II})$.

exergonic and the high barrier for the backward reaction (25.7 kcal/mol) should make the reaction irreversible.

4.1.3. Breaking the N–O bond and forming N_2O

To form the nitrous oxide (N_2O) one of the two N–O bonds in the five-membered ring has to be broken. Intuitively, the best of the two bonds to break is the N1–O3 bond bridging the heme a_3 iron and Cu_B , forming a N_2O coordinated with its primary nitrogen (N1) to the heme iron. When N_2O has left, an intermediate with a bridging oxo (Fe(III)–O–Cu(II)) would be formed in a thermoneutral reaction with respect to the five membered ring. All attempts to break any of the two N–O bonds would initially form a $Cu(II)$ –O $^{2-}$ species, which is very high in energy. As expected, stretching the N–O bond in the calculations raised the energy too much to give a reasonable barrier for the reaction to proceed. A second possible pathway would be a mechanism where O3 coordinates to the heme iron either before or simultaneously with the breaking of the N–O bond. The concerted type of reaction where the N1–O3 binds in a side on fashion to the heme a_3 iron in the transition state also gave far too high energies for the reaction to proceed. In a corresponding stepwise reaction the five-membered ring could first change its coordination to the heme iron from N1 to an O3 coordinating to the heme iron and bridging the two metal ions, and then break the N1–O3 bond. However, the intermediate with an O3 bridging the two metal ions is 12 kcal/mol less stable compared to the original five-membered ring shown in Fig. 5.

All attempts to break the N–O bond forming nitrous oxide and a Fe(III)–O– Cu_B (II) intermediate were unsuccessful. Thus, something has to change in the active site for the reaction to continue. In the reduction of NO, two electrons and two protons are transferred to the binuclear center, and since the reaction cannot go via the pathways described above it is very plausible that a proton or an electron enters the binuclear center at this stage. An extra electron would most probably reduce the ferric heme, which would neither change the N–O bond strength to a large extent nor make the product $Cu(II)$ –O $^{2-}$ Fe(II)– N_2O significantly more stable. Therefore, it is assumed that a proton enters the binuclear center at this stage. O3 and N2 in the five-membered intermediate have similar proton affinities (268.5 and 267.7 kcal/mol), whereas a protonation of O4 or N1 is 6.0 and 10.0 kcal/mol less stable, respectively. The five-membered ring will therefore be protonated at O3 and N2 to a similar extent at equilibrium. Protonating N2 will not lead directly to a reactive intermediate, but with a second protonation at O4 an isomer of hyponitrous acid (ONN(H)OH) would be formed which could isomerize to N_2O and H_2O by an internal proton transfer. The latter mechanism is discussed below in Section 4.6.

If O3 is protonated, see Fig. 6, the product formed after the N–O bond is cleaved changes to a Cu_B (II)–OH and Fe(III)– N_2O . The optimized transition state of this reaction step can be seen in Fig. 7. The N1–O3 bondlength is 2.06 Å and both the N1 coordination to the heme iron and the O4 coordination to Cu_B are weakened. The N–N–O angle is

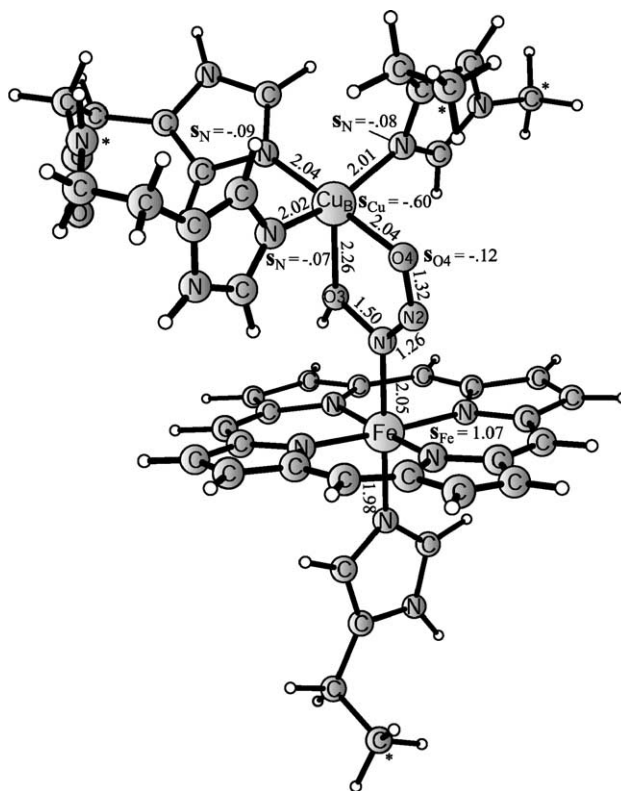


Fig. 6. The protonated five-membered ring bridging the heme Fe(III) and Cu_B (II).

increased to 142.2° in the transition state, from 120.6° in the protonated five-membered ring. The spin population on N1–N2–O4 is 0.02, 0.01, -0.06 showing that a closed shell nitrous oxide starts to form when the N1–O3 bond is broken heterolytically.

The oxidation states of the binuclear center are unaltered (Fe(III)– N_2O and $Cu(II)$ –OH), with spin populations of 1.06 and -0.60 , respectively. The reaction is exergonic by 12.8 kcal/mol with an intrinsic barrier of 15.5 kcal/mol relative to the protonated five-membered ring.

The coordination of the nitrous oxide formed is very weak which is shown geometrically in a very long Fe–N1 bond distance of 2.32 Å. The bond strength between Fe(III) and N_2O has been calculated to be 2.8 kcal/mol and the nitrous oxide is bound in a shallow enthalpy minimum. The latter calculations were done for a small model described in Section 2, where only the heme side of the binuclear site is incorporated, whereas the Cu_B center with its histidine ligands is excluded. Adding the release of entropy when N_2O leaves would drive this step of the reaction forward making it exergonic by 7.2 kcal/mol. After N_2O has left its coordination to the heme iron, the hydroxyl group will form a bridge between the heme iron and Cu_B without a barrier. The release of N_2O together with the formation of a Fe(III)–OH– Cu_B (II) is exergonic by 15.3 kcal/mol relative to Fe(III)– N_2O and Cu_B (II)–OH.

4.1.4. The reduction of the hydroxyl group to water

After nitrous oxide is formed and has left the active site, the latter has to be reduced back to the fully reduced state while

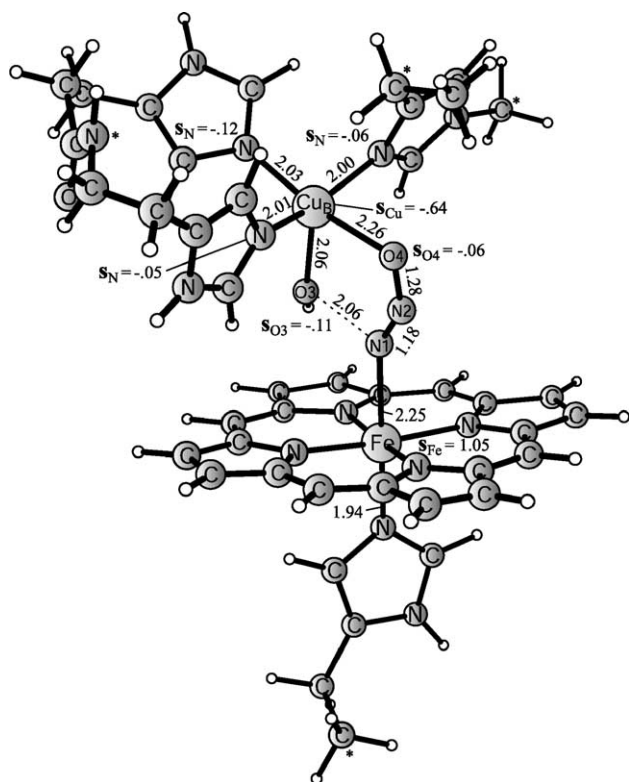


Fig. 7. The transition state of the N1–O3 bond cleavage (TS2a), forming N_2O and a hydroxyl group bound to Cu_B .

forming water to be ready to begin a new catalytic cycle. In this process, the remaining proton and the two electrons used in the reaction are transferred to the binuclear center.

The first electron, reducing the $Fe(III)-OH-Cu_B(I)$ intermediate is transferred from heme *b*, and the calculated electron affinity (EA) for this intermediate is 120.7 kcal/mol. This EA is assumed to be high enough to oxidize heme *b*. The electron transfer reduces Cu_B forming an $Fe(III)-OH-Cu_B(I)$ intermediate. The reduction decreases the positive charge of the binuclear center and the proton affinity (PA) is raised to 278.5 kcal/mol. This PA can be compared to the PA of the five-membered ring (268.5 kcal/mol), the transfer of the second proton will thus be 10.0 kcal/mol more favorable.

The second protonation, forming $Fe(III)-H_2O-Cu_B(I)$, raises the positive charge of the binuclear center and thereby the electron affinity is increased to 114.1 kcal/mol. By comparing the latter with the EA of the $Fe(III)-OH-Cu_B(II)$ intermediate, which is 120.7 kcal/mol, the second electron transfer will be 6.6 kcal/mol less exergonic. Thus, the relative electron and proton affinities can be calculated, while the energetics of the transfers of protons and electrons has to be estimated by comparison to experiments, see Section 4.3.

The release of water in the $Fe(II)-OH_2-Cu_B(I)$ intermediate is exergonic by 6.8 kcal/mol. Furthermore, the barrier for the water to lose its coordination can be expected to be low, since the process is exergonic and the oxidation state of the binuclear center is unaltered. However, the water molecule is unbound also in the ferric state of the heme ($\Delta G = -6.7$ kcal/mol), which

implies that there will be a competition between the release of water and reduction of heme a_3 . The almost identical electron affinities for $Fe(III)-OH_2-Cu_B(I)$ and $Fe(III)-Cu_B(I)$ (114.1 kcal/mol) imply that both intermediates can accept an electron with similar energetics. The order in which the electron is transferred and the water leaves will not be particularly important for the interpretation of the resulting reaction mechanism. The energetics for the overall reaction is discussed in Section 4.4.

The calculated electron and proton affinities in this section are used to evaluate at which other stages the electrons and protons could enter the catalytic cycle, which is discussed below in Sections 4.2 and 4.3.

4.2. Case B—the first electron enters before the N–O bond is broken

In the second mechanism of the NO reduction investigated, the first electron transfer to the binuclear site is assumed to occur directly after the protonation of the five-membered ring. The reduction will not change the entire mechanism, but only the steps from the protonated five-membered ring intermediate to $Fe(III)-OH-Cu_B(I)$ will differ from case A. See Fig. 2 for an overview of the investigated reaction mechanisms. This mechanism is the one favored in the present study.

4.2.1. Breaking the N–O bond and forming N_2O

The electron affinity (EA) of the protonated five-membered ring is 113.8 kcal/mol, to be compared with the EA of the $Fe(III)-OH_2-Cu_B(I)$ intermediate which is 114.1 kcal/mol. Since the binuclear site is reduced back to the fully reduced state ($Fe(II)-Cu_B(I)$) at the end of the catalytic cycle, the similar EAs imply that the protonated five-membered ring is equally able to oxidize heme *b*. The oxidation states of the metal ions in the reduced protonated five-membered ring intermediate is $Fe(II)$ and $Cu_B(II)$, the latter having a spin population of -0.58 (Fig. 8).

In case B, the N1–O3 bond is broken in a similar way as in case A, but the barrier is decreased to 10.0 kcal/mol with respect to the preceding intermediate, which is the reduced protonated five-membered ring. In the transition state the N1–O3 bond is 2.18 Å. The Cu_B-O4 bond is elongated to 2.25 Å, whereas the N1–N2–O4 angle has increased from 121.4° to 141.4°, see Fig. 9. The product of the reaction is a hydroxide coordinated to $Cu_B(II)$ and a nitrous oxide coordinated to $Fe(II)$, the reaction step is exergonic by 17.3 kcal/mol. The bond strength between $Fe(II)$ and N_2O has been calculated to be 3.7 kcal/mol. Adding the release of entropy when the N_2O molecule leaves its coordination makes the reaction exergonic by 6.3 kcal/mol. The nitrous oxide leaves its coordination without an enthalpy barrier.

After the N_2O has left the active site, the hydroxyl group bound to $Cu_B(II)$ could in principle form a bridge between the heme iron and Cu_B similarly with case A. There is, however, a low barrier since both metal ions change their oxidation state in this step, $Fe(II)$ being oxidized to $Fe(III)$ and $Cu_B(II)$ reduced to $Cu_B(I)$, respectively. The barrier for this reaction is

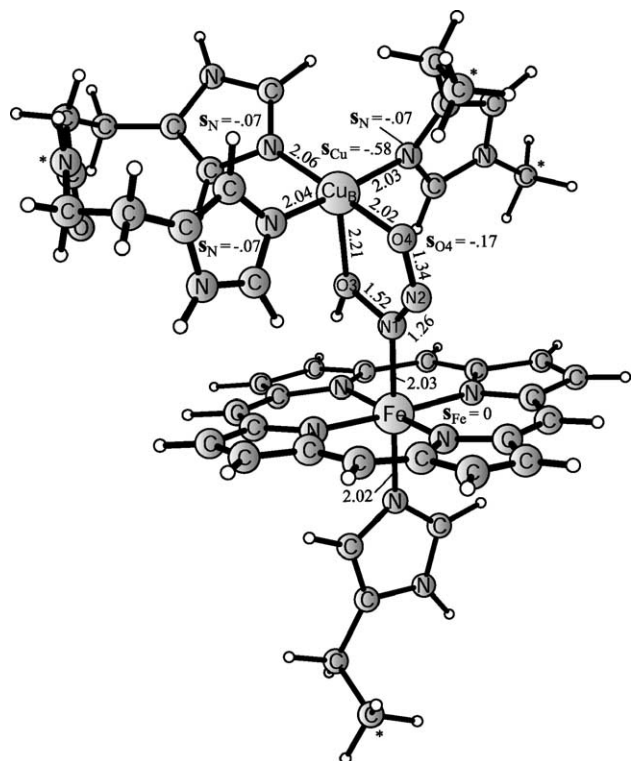


Fig. 8. The five-membered ring with N1 coordinating to a reduced heme Fe(II) and O3 and O4 coordinating to Cu_B(II).

only 1.2 kcal/mol. However, this reaction step will compete with the change in spin state of the five coordinated heme from low to high spin. In the high spin case the barrier is only 6.1 kcal/mol, and the reaction would still be very fast. In TS3b the Cu_B–OH and Fe–OH bond distances are 1.95 and 2.41 Å, respectively. The spin population on Cu_B is reduced slightly to –0.54, whereas the spin population on the heme iron has started to appear and is –0.05. Releasing N₂O and forming Fe(III)–OH–Cu_B(I) is exergonic by 17.6 kcal/mol relative to the Fe(II)–N₂O and Cu_B(II)–OH intermediate. The free energy profile of the reaction mechanism in case B is discussed in Section 4.5.

The remaining reaction steps in the catalytic cycle are identical to those in case A discussed above in Section 4.1, see Fig. 2 for an overview of the reaction mechanisms described in cases A–D.

4.3. Energetics of the proton and electron transfers

The results from the calculations on the two mechanisms (cases A and B) presented above contain important information about the mechanism and the energetics of the NO reduction in a terminal oxidase. However, the energetics of the electron and proton transfers are difficult to calculate accurately, but are of large importance for the energetics and thereby for the discrimination between the different cases. For example, the calculated intrinsic barriers for the rate limiting step are 15.5 (TS2a) and 10.0 kcal/mol (TS2b) before (case A) and after the electron transfer (case B), respectively. However, since the total barrier of the rate limiting step is not solely depending on the

barrier of breaking the bond, but depends also on the energetics of the entering protons and electrons, these energies are needed to evaluate which path is most likely. Furthermore, in cases C and D the rate limiting barriers actually consist of the transfer of the protons and electrons as will be shown below in Sections 4.6 and 4.7.

In the present section, a combination of experimental data and calculated relative energies are used to determine the energetics of the electron and proton transfers. Thereby, free energy surfaces for the whole catalytic cycles of the reaction mechanisms (cases A and B) described in Sections 4.1 and 4.2 are obtained, see Sections 4.4 and 4.5 below. It should be noted that there are uncertainties in both the experimental and calculated values, and the energetics for the electron and proton transfers should therefore be viewed qualitatively.

The experimental midpoint reduction potentials for a ba₃-oxidase have been determined to $E_{m1} = -0.02 \pm 0.01$ and $E_{m2} = 0.16 \pm 0.04$ V for heme *b*, and correspondingly to $E_{m1} = 0.13 \pm 0.04$ and $E_{m2} = 0.22 \pm 0.03$ V for heme *a*₃, referring to the Ag/AgCl/3 M KCl reference electrode at 5 °C [26]. Using the main midpoint reduction potentials, E_{m1} and E_{m2} for heme *b* and heme *a*₃, respectively, the approximate ΔG for an electron transfer between heme *b* and *a*₃ can be calculated. The obtained $\Delta G = -5.5$ kcal/mol is assumed to correspond to the energetics for the second electron transfer in the investigated reaction mechanism, that is the reduction of Fe(III)–OH₂–Cu_B(I) to Fe(II)–OH₂–Cu_B(I), while oxidizing heme *b*. Since the relative electron affinities can be calculated for all intermediates, the energetics of the

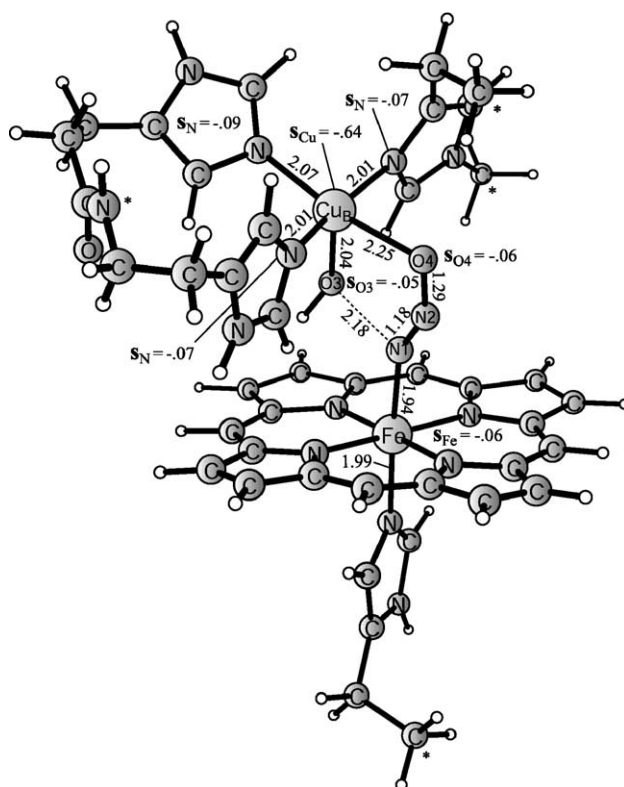


Fig. 9. The transition state of the N1–O3 bond cleavage (TS2b), forming N₂O and a hydroxyl group bound to Cu_B.

second electron transfer will determine the energetics of all other possible electron transfers during the catalytic cycle. The EA of $\text{Fe(III)}\text{--OH}_2\text{--Cu}_B\text{(I)}$ is 114.1 kcal/mol and corresponds to an electron transfer exergonic by 5.5 kcal/mol. The EA of the ferric heme *b* is thus estimated to be 108.5 kcal/mol, which will be used as a reference to evaluate the energetics of the electron transfers in cases A–D.

Furthermore, the potential for the reduction of two nitric oxides to nitrous oxide and water according to Eq. (1) in section V is E'_0 (pH=7.0)=1.177 V (SHE), which corresponds to $\Delta G'_0 = -54.3$ kcal/mol. This reduction potential can be transferred from the standard hydrogen electrode (SHE) reference to heme *b*, the latter having the reduction potential $E_0 = 0.19$ V [26]. Taking the electrons from heme *b* gives an E''_0 (pH=7.0)=0.989 V for the reduction of NO, which corresponds to a $\Delta G = -45.6$ kcal/mol. Since only the relative energies for the proton transfers can be calculated, the experimental ΔG of the overall reaction is used together with the exergonicity of the electron transfers described above, to determine the energetics of the two proton transfers from the bulk. The proton affinity of the bulk was in this way estimated to be 281.0 kcal/mol, which is used as a reference, determining the energetics of the proton transfers in cases A–D. The transfers of protons to the binuclear center during the reaction appear to be endergonic and will turn out to be crucial for the barrier height of the rate limiting step. The energies obtained for the proton and electron transfers are used in the discussion of the reaction mechanisms below.

To compare the calculated energetics with the reduction potential determined according to the standard state of the reactants and products, the gas phase energies are used for NO and N_2O . Furthermore, the ΔH_{soliv} for water is taken from experiments.

The experimental NO-consumption turnover number has been determined to 0.06 ± 0.01 mol NO/mol $\text{ba}_3 \times \text{s}$ [4], which corresponds to a rate limiting barrier of 19.5 kcal/mol using transition state theory. The experimental barrier for the rate-limiting step is used to probe the investigated mechanisms (A–D) to determine which one of them is most plausible. Furthermore, the oxidation rate of heme *b*, which is 0.04 s^{-1} [4], has been shown to be very similar to the turnover rate, implying that the electron transfer can be associated with the rate limiting step of the reaction. It has also been shown that the reduction rate of heme *b* increases with increasing NO concentration [4].

In the sections below, free energy profiles for cases A and B are constructed, including the energetics of the electron and proton transfers. The dashed barriers in the energy profiles presented below correspond to the barriers of the proton transfers which have not been calculated. Furthermore, the barriers for the leaving of the neutral ligands N_2O and H_2O are dashed. These barriers are expected to be low since the processes are exergonic and the oxidation states of the metal ions are unaltered. As will be seen in the following sections the most favored mechanism turns out to be the one in case B.

4.4. Case A: the free energy profile of the NO reduction

In this section the free energy surface of the NO reduction in case A is analyzed and the energetics of the proton and electron transfers are used to calculate a free energy surface as shown in Fig. 10.

From the free energy profile of the reaction mechanism it can be seen that there are two transition states in which covalent bonds are formed or broken (TS1, TS2a). In TS1 the N–N bond is formed and the reaction has an enthalpy barrier of 4.0 kcal/

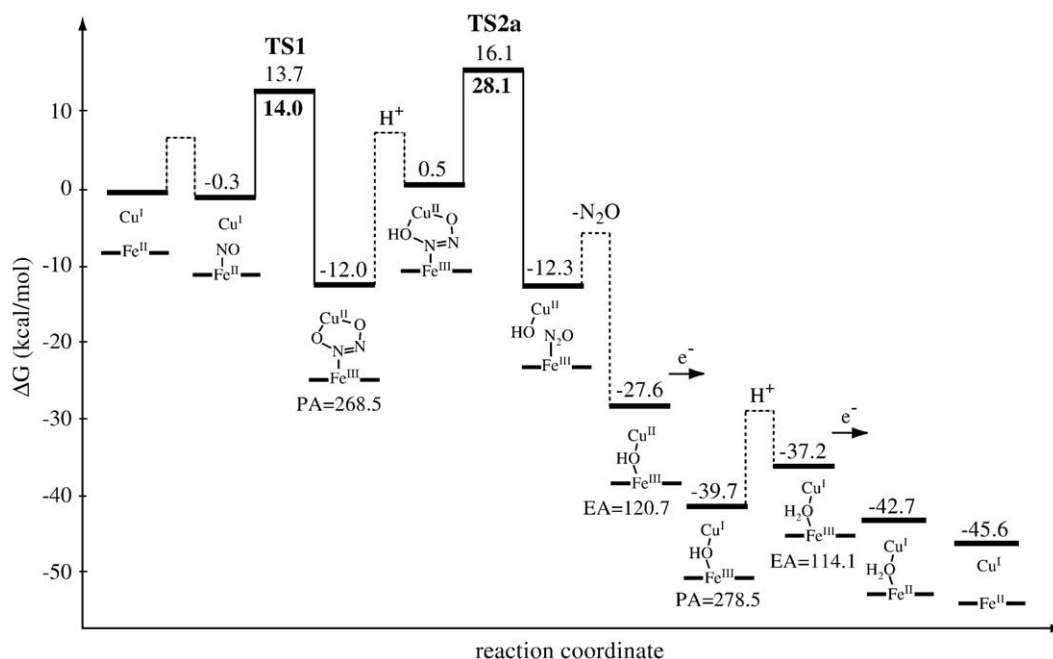


Fig. 10. Case A: the free energy profile for the reduction of nitric oxide to nitrous oxide. The N–O bond is broken in a rate limiting step directly after the protonation of the five-membered ring.

mol, the addition of the entropy cost of forming the transition state makes the free energy barrier 14.0 kcal/mol. The barrier is thus very sensitive to the entropy cost of bringing NO from the bulk to the transition state. The entropy cost will depend on the concentration of NO, the lowest cost being when the active site is saturated with the substrate. The barrier of TS1 is thus likely to be lower than 14.0 kcal/mol.

As described in Section 4.1 (Case A) the five-membered ring (Fig. 5) has to be protonated to break the N–O bond and form nitrous oxide. By comparing the proton affinity at O3 of the five-membered ring (268.5 kcal/mol) with the PA of the bulk (281.0 kcal/mol, see Section 4.3), the first proton transfer is estimated to be endergonic by 12.5 kcal/mol. Together with the intrinsic barrier for breaking the N1–O3 bond, the total barrier is 28.1 kcal/mol (Fig. 10), which clearly is too high compared to the experimental barrier of 19.5 kcal/mol. The reaction will thus most likely not go via this reaction path.

The formation of nitrous oxide is an exergonic process which together with the endergonic protonation of the five-membered ring, makes the reaction exergonic by 0.3 kcal/mol compared to the resting state, see Fig. 10. N₂O will leave the active site by losing its weak coordination to the ferric heme iron. The hydroxide coordinated to Cu_B(II) will then bridge the two metal ions without a barrier in a step exergonic by 15.3 kcal/mol. At this stage the first electron transfer occurs. The EA of Fe(III)–OH–Cu_B(II) is 120.7 kcal/mol, which should be compared to the reference EA of heme *b*. The latter being 108.5 kcal/mol gives an exergonic electron transfer to Fe(III)–OH–Cu_B(II) by 12.1 kcal/mol, see Fig. 10.

Since the rate limiting barrier in case A turned out to be too high (28.1 kcal/mol) compared to experiments (19.5 kcal/mol) and the remaining part of the free energy profile going from Fe

(III)–OH–Cu_B(I) to the fully reduced active site is identical with the reaction mechanism in case B, the rest of the reaction steps in the free energy profile are discussed below in Section 4.5.

4.5. Case B: the free energy profile of the NO reduction

The energetics of the mechanism in case B can be seen in Fig. 11. The energetics for the proton and electron transfers are determined in the same way as described above in Section 4.3.

In case B the first electron transfer occurs directly after the first protonation. The protonated five-membered ring has an EA=113.8 kcal/mol, which is very similar to the EA of the Fe(III)–OH₂–Cu_B(I) intermediate (114.1 kcal/mol). The similar EAs for the protonated five-membered ring and Fe(III)–OH₂–Cu_B(I) imply that both intermediates should be equally able to oxidize heme *b*. Comparing the EA of the protonated five-membered ring with the EA of heme *b*, the latter being 108.5 kcal/mol, makes the first electron transfer in case B exergonic by 5.3 kcal/mol. The ferric heme *a*₃ is reduced to ferrous by the incoming electron, which decreases the intrinsic barrier of the N1–O3 bond cleavage from 15.5 kcal/mol in case A to 10.0 kcal/mol in case B, as discussed in Sections 4.1 and 4.2. The total barrier will thus be 17.3 kcal/mol relative to the resting state, which is the five-membered ring, see Fig. 11.

In both cases A and B, the rate limiting step is the cleavage of the N1–O3 bond. In case B, the barrier of TS2b is 17.3 kcal/mol which is close to the corresponding experimental barrier of 19.5 kcal/mol, whereas in case A, the barrier is much too high (28.1 kcal/mol). It is interesting to note that the barrier of TS2b is independent of the energetics of the electron transfer since both a proton and an electron are transferred before the bond is broken. The latter is valid as long as the five-membered ring is the resting

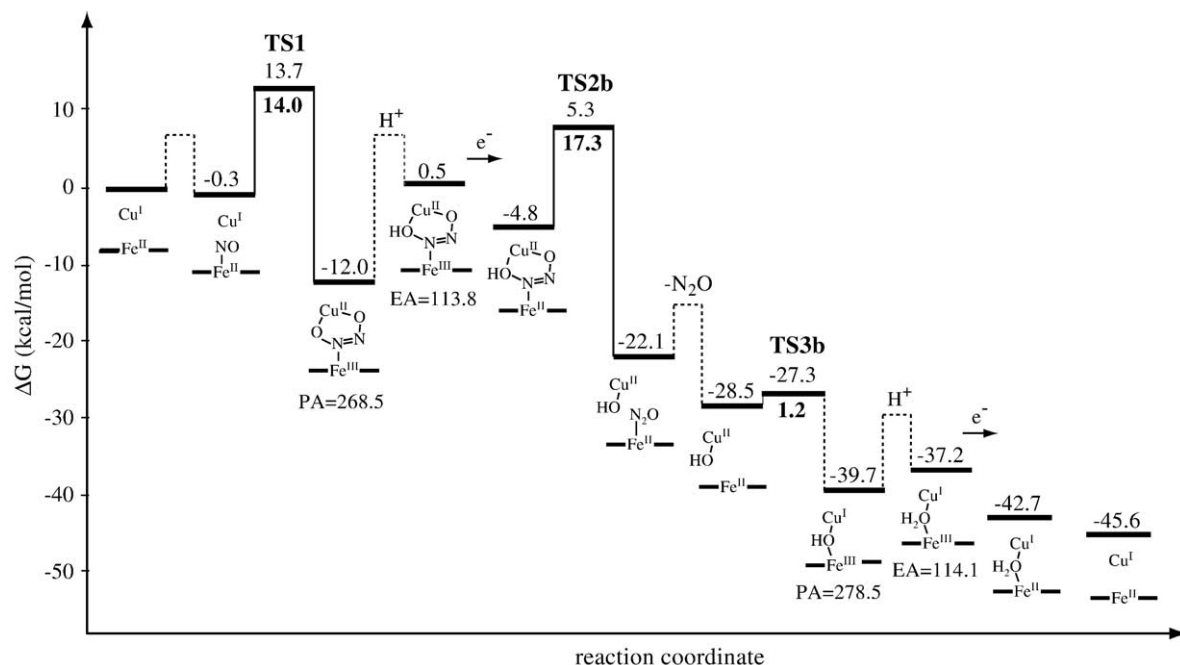


Fig. 11. Case B: the free energy profile for the reduction of nitric oxide to nitrous oxide. In this case, the N–O bond is not broken before both a proton and an electron have been transferred to the binuclear site.

state. The height of TS2b is thus only dependent on the ΔG of the overall reaction. Furthermore, since the intrinsic barrier of TS2b is lower (10.0 kcal/mol) than the corresponding TS2a in case A (15.5 kcal/mol), the two barriers would only be equal if the first electron transfer is endergonic by 5.5 kcal/mol, which means that the electron transfer to Fe(III)–OH₂–Cu_B(I) should be endergonic by 5.3 kcal/mol, compared to exergonic by 5.5 kcal/mol as calculated from the experimental reduction potentials. Thus, the error in the experimental reduction potentials has to be unlikely large to favor case A compared to case B.

In case B, the electron transfer occurs before the rate limiting step, whereas the experimental findings show that the oxidation rate of heme *b* is similar to the rate limiting step of the reaction. However, the electron transfer is reversible, and since the reduced protonated five-membered ring is not the resting state, but the unprotonated five-membered ring (Fe(III) and Cu_B(II)), the equilibrium will be shifted toward a reduced heme *b*. The electron transfer will thus not be detectable until the rate limiting barrier of TS2b has been passed. On the other hand, the observation that the oxidation rate of heme *b* increases with an increased NO concentration, implies that TS1 should be rate limiting. The latter does not fit with the calculated energy profile and it seems unlikely that such a low enthalpy barrier should be rate limiting with a rate corresponding to a barrier of 19.5 kcal/mol.

After the N1–O3 bond has been broken, the N₂O formed is bound to Fe(II). The bond strength of N₂O to Fe(II) is 3.7 kcal/mol, and the increase in entropy when N₂O leaves its coordination makes the reaction exergonic by 6.3 kcal/mol. The Fe(II) Cu_B(II)–OH intermediate formed is very unstable and the bridging Fe(III)–OH–Cu_B(I) intermediate should be formed rapidly, see Fig. 11. The Fe(III)–OH–Cu_B(I) intermediate has a proton affinity of 278.5 kcal/mol, which is 2.5 kcal/mol lower than the PA of the bulk (281.0 kcal/mol). The second proton transfer will thus be endergonic by 2.5 kcal/mol.

In oxidized NOR, the presence of a stable μ -oxo bridge between the ferric heme and non-heme iron has been proposed [27]. In a *ba*₃-oxidase, the corresponding intermediate is an Fe(III)–O–Cu_B(II). However, the latter has a high proton affinity (289.4 kcal/mol) compared to the bulk (281.0 kcal/mol) and the following reduction by an electron coming from heme *b* is exergonic by 12.1 kcal/mol, see Fig. 10. The Fe(III)–O–Cu_B(II) intermediate is thus quite unstable and would most likely not be formed during the reduction of NO in a *ba*₃-oxidase.

The proton transfers discussed above are endergonic by at most 12.5 kcal/mol, and whether this is reasonable can be evaluated by comparison to other proton transfers in similar systems. The PA of a Fe(III)–OH HO–Cu_B(II) intermediate in the O₂ reduction in cytochrome *c* oxidase has been calculated, and can be compared to the corresponding intermediate in the present study, Fe(III)–OH–Cu_B(I). These two intermediates have the same total charge, and in both cases the proton is transferred to a hydroxide coordinating to a ferric heme. In the Fe(III)–OH HO–Cu_B(II) intermediate, to which the proton transfer is expected to be exergonic [28], the PA is 289 kcal/mol (Blomberg, M.R.A., unpublished data). As discussed above the Fe(III)–OH–Cu_B(I) intermediate has a PA=278.5 kcal/mol.

The proton transfer to Fe(III)–OH–Cu_B(I) being endergonic by 2.5 kcal/mol fits rather well with the 10 kcal/mol lower proton affinity for this intermediate and an exergonic proton transfer to the Fe(III)–OH HO–Cu_B(II) intermediate in cytochrome *c* oxidase.

Protonating Fe(III)–OH–Cu_B(I) raises the EA to 114.1 kcal/mol, which corresponds to the electron transfer being exergonic by 5.5 kcal/mol according to experiments as discussed above, see Fig. 11. After the second electron transfer the binuclear center is reduced back to the fully reduced state. The water molecule is, as mentioned in Section 4.1, only weakly coordinated to both the ferrous and ferric heme, and leaving the binuclear center could thus compete with the reduction of the latter. The order of these steps will however not affect the interpretation of the free energy profile, since the EA is hardly affected by the presence of the water.

In Sections 4.6 and 4.7 below two alternative mechanisms, C and D, for the NO reduction are discussed. These mechanisms differ in the position of protonation compared to cases A and B and also in the need of being doubly protonated forming an isomer of hyponitrous acid before the N–O bond can be broken forming nitrous oxide.

4.6. Case C: an alternative protonation of the five-membered ring

In Section 4.1, it was concluded that the proton affinity for the five-membered ring is very similar at O3 and N2, which implies that they will be protonated to a similar extent. In this section, a mechanism following the protonation of N2 has been investigated and the resulting free energy profile is shown in Fig. 12. Similarly to what has been shown above the proton transfers are endergonic also in this reaction path. The protonation of the five-membered ring at N2 does not lead directly to a reactive intermediate as the protonation of O3 did, see Section 4.1. However, by further addition of one electron and proton the five-membered ring will be reduced to hyponitrous acid, which is known to isomerize to water and nitrous oxide in solution (Angeli's salt). An overview of the reaction mechanisms investigated in the present study can be seen in Fig. 2.

4.6.1. Formation of hyponitrous acid coordinating to the binuclear center

The proton affinity of N2 is 267.7 kcal/mol, which can be compared to the PA of the bulk (281.0 kcal/mol). This means that a proton transfer to N2 in the five-membered ring is endergonic by 13.3 kcal/mol. The protonation of N2 shortens the N1–O3 bond length inducing some double bond character which weakens the coordination between Cu_B(II) and O3.

Furthermore, the protonation of the five-membered ring at N2 raises the electron affinity to 111.0 kcal/mol, which by comparison to the EA of heme *b* (108.5 kcal/mol) gives an electron transfer exergonic by 2.4 kcal/mol. The electron transfer reduces the ferric heme iron to ferrous and in addition the proton affinity for O4 increases to 261.6 kcal/mol. The second proton transfer is thus endergonic by 19.4 kcal/mol by comparison to the PA of the bulk (281.0 kcal/mol). After the

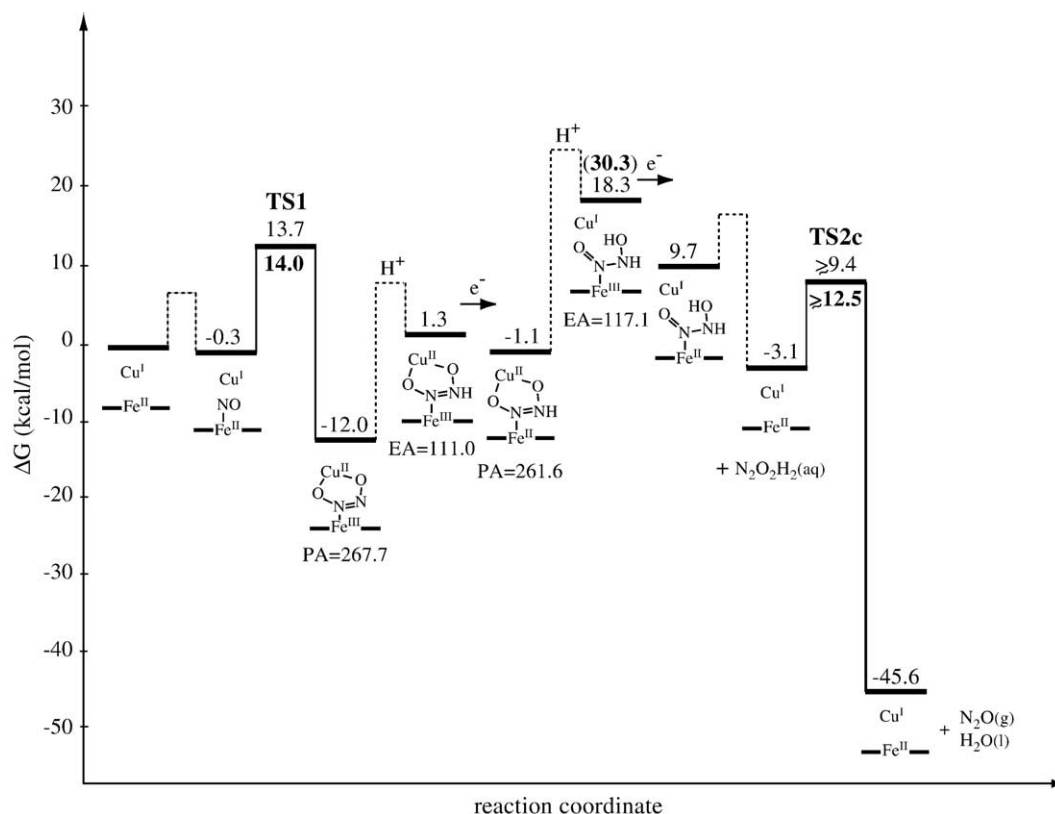


Fig. 12. Case C: the similar proton affinities at O3 and N2 in the five-membered ring implies that both positions should be protonated to similar extent. In case C, the mechanism where N2 is protonated is investigated. Further reduction and protonation leads to the formation of hyponitrous acid which can isomerize to N₂O and H₂O by a proton transfer from N2 to O4.

second protonation, a neutral hyponitrous acid is formed and in this step an electron is transferred from Fe(II) to Cu_B(II) while O3 and O4 loses their coordination to Cu_B. The hyponitrous acid coordinated between Fe(III) and Cu_B(I) is 30.3 kcal/mol less stable than the resting state, which is the five-membered ring, see Fig. 12. This means that the rate limiting barrier is at least 30.3 kcal/mol relative to the resting state and probably higher since there should be at least a small barrier for the proton transfer, which makes the mechanism in case C very unlikely. The electron affinity is raised to 117.1 kcal/mol by the second protonation, which by comparison to the EA of the bulk (108.5 kcal/mol) makes the second electron transfer exergonic by 8.6 kcal/mol.

Hyponitrous acid could then either leave the active site, which is exergonic by 12.8 kcal/mol, or alternatively isomerize at the active site. The energetics of hyponitrous acid leaving the active site for the solution is somewhat uncertain since the dielectric continuum model describes the hydrogen bonds in water quite poorly. However, this step is not very important for the interpretation of the free energy surface. The isomerization of N₂O₂H₂ in solution is exergonic by 42.5 kcal/mol. The proton transfer is assisted by two water molecules and has a barrier of 12.5 kcal/mol. The entropy cost of forming the transition state in bulk water is hard to estimate and the barrier is given with the entropy cost of going from a reactant complex where the waters are already in the right positions. This barrier is presumably slightly underestimated and a few kcal/mol

should probably be added. A presumed proton transfer in the active site should also most likely be water assisted.

The largest difference comparing case C with cases A and B is that in case C at least the two protons and one of the electron have to be transferred before the N–O bond can be broken forming N₂O. This means that two endergonic proton transfers have to occur before nitrous oxide can be formed, the latter step releasing a large amount of energy which should drive the reaction forward.

4.7. Case D: protonation of the Fe(II)–NO–Cu_B(I) intermediate

In the fourth reaction path, a protonation already at the stage when NO becomes coordinated to the binuclear site is investigated. This mechanism would resemble the mechanism proposed for NO reduction in the fungal P450 type of NOR. In the fungal NOR a nitric oxide is coordinated to a P450 type of heme and has been proposed to be reduced directly by an addition of H⁺ from the cofactor NADH [29]. The coordinated HNO is then proposed to be further protonated at the oxygen, followed by the attack of a second NO forming an isomer of hyponitrous acid (ONN(H)OH). The latter can isomerize to nitrous oxide and water by a proton transfer, either at the P450 heme or in solution. The mechanism of NO reduction in a P450 NOR has been investigated theoretically by Vincent et al. [30]. An alternative route could be if HNO is released from the active site since HNO can react with a second HNO in solution

forming N_2O and H_2O [25]. The free energy surface of case D can be seen in Fig. 13.

4.7.1. Formation of $\text{Fe(II)}\text{--HNO}\text{--Cu}_B(\text{I})$

$\text{Fe(II)}\text{--NO}\text{--Cu}_B(\text{I})$ has a PA of 262.6 kcal/mol, which by comparison to the PA of the bulk (281.0 kcal/mol) makes a protonation of NO coordinated to the reduced binuclear center endergonic by 18.4 kcal/mol. The heme iron, which was only partly oxidized while binding NO, is now fully oxidized to Fe (III) with a spin population of 1.01. Furthermore, Cu_B is oxidized to $\text{Cu}_B(\text{II})$ with a spin population of -0.56 . As a consequence HNO has been reduced to HNO^- with a spin population of -0.61 and -0.48 for N1 and O3, respectively. The very endergonic proton transfer results in a too high energy for the HNO to leave the active site since this process is calculated to be endergonic by 5.0 kcal/mol relative to the bound HNO, which corresponds to 23.4 kcal/mol relative to the resting state, which has NO bound in the reduced binuclear center. On top of this, the barrier for the dimerization of two HNO must be added which makes this reaction mechanism very unlikely. However, it should be noted that the free energy of binding HNO to the binuclear center is a bit uncertain since the dielectric continuum model describes the hydrogen bonds in water quite poorly.

4.7.2. Formation of hyponitrous acid

Following the mechanism proposed for the P450 type of NOR a second NO can attack the coordinated HNO molecule forming a five-membered ring. The potential energy surface forming the N–N bond is very flat similar to the corresponding formation of an N–N bond in cases A and B (TS1) described in Sections 4.1 and 4.2. Scanning the bond distance gives an approximate transition state with an N1–N2 distance of 2.20 Å. The spin populations on N1, O3, N2 and O4 are -0.39 , -0.31 , 0.43 and 0.17 , respectively, which show that some spin density is transferred from the coordinating to the attacking NO. The intrinsic barrier of TS1d is 13.0 kcal/mol. In the product both oxygens coordinate to $\text{Cu}_B(\text{II})$ and the ring becomes planar as

N1 loses its coordination to the ferric heme a_3 . The reaction is exergonic by 7.2 kcal/mol with respect to HNO coordinating to the binuclear center and a free NO. The total barrier will thus be 31.1 kcal/mol relative to the resting state with one free NO and one NO coordinated to the reduced binuclear center, see Fig. 13.

The barrier of TS1d lies almost 15 kcal/mol above the barrier of TS2b in case B. Furthermore, the formation of the five-membered ring with a protonated N1 is thermodynamically unfavored by 10.4 kcal/mol compared to a protonation at O3, see Fig. 6. Thus, it can be concluded that the reaction path in case D is energetically less favored than the one of case B and the reaction will most likely not go via this path.

The continuation of the reaction mechanism in case D should be very similar to case C, described above in Section 4.6. The major difference between the mechanisms in cases C and D is the coordination, and as long as N2 does not coordinate to the heme iron, mechanism D will be energetically less favored than case C. The mechanism in case D was therefore not further investigated in the present study. See Fig. 2 for an overview of the reaction mechanisms in cases A–D and Fig. 14 for a summary of the energy profiles described in Sections 4.4–4.7.

5. Conclusions

The mechanism of the reduction of two molecules of nitric oxide to nitrous oxide and water in a ba_3 -oxidase has been investigated. During one catalytic cycle two electrons and two protons are needed to form nitrous oxide and water, and finally regenerate the fully reduced active site ($\text{Fe(II)}\text{--Cu}_B(\text{I})$). The questions addressed in the present study are concerned with the mechanism of formation of nitrous oxide, and also at which stages in the reaction sequence the electrons and protons are transferred. The mechanisms investigated are shown schematically in Fig. 2 and the free energy diagrams are summarized in Fig. 14.

The experimental reduction potentials for heme b and a_3 were used to estimate the energy of the second electron transfer. Because the relative electron affinities of different intermediates have been calculated, the calibration of the energetics of one electron transfer will determine the remaining ones. Similarly, the ΔG value for the overall reaction, which was calculated from the reduction potential for the reduction of two NO to N_2O and H_2O , was used to determine the energetics of the two proton transfers. The latter were shown to be quite endergonic and thereby crucial for the barrier height of the rate-limiting step.

In the two main reaction mechanisms investigated, A and B, the rate limiting step corresponds to the breaking of the N–O bond. The intrinsic barriers for this step are calculated to be 15.5 and 10.0 kcal/mol for cases A and B, respectively. The rate limiting barrier calculated from the experimental turnover rate is 19.5 kcal/mol. The intrinsic barriers are thus too low compared to experiments. However, to break the N–O bond O3 has to be protonated. In case A, the N–O bond is broken directly after the protonation, whereas in case B, an electron transfer to the protonated five-membered intermediate (Fig. 6) precedes the breaking of the bond. The preferred reaction path will thus depend on the energetics of the proton and electron transfers to

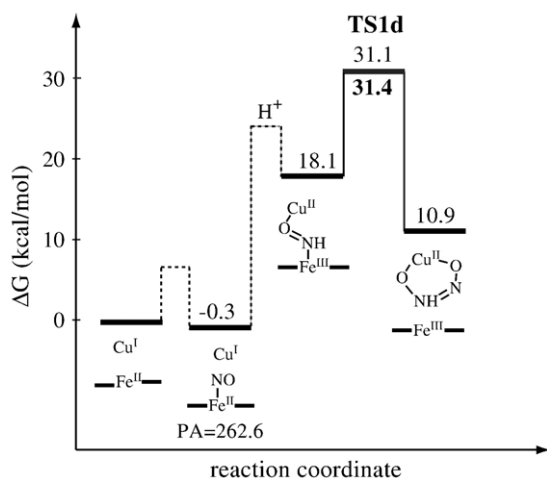


Fig. 13. Case D: protonation of NO coordinated to the heme iron forming HNO. The latter is attacked by a second NO forming ON(H)NO which can be protonated and isomerize to N_2O and H_2O by a proton transfer from N1 to O3.

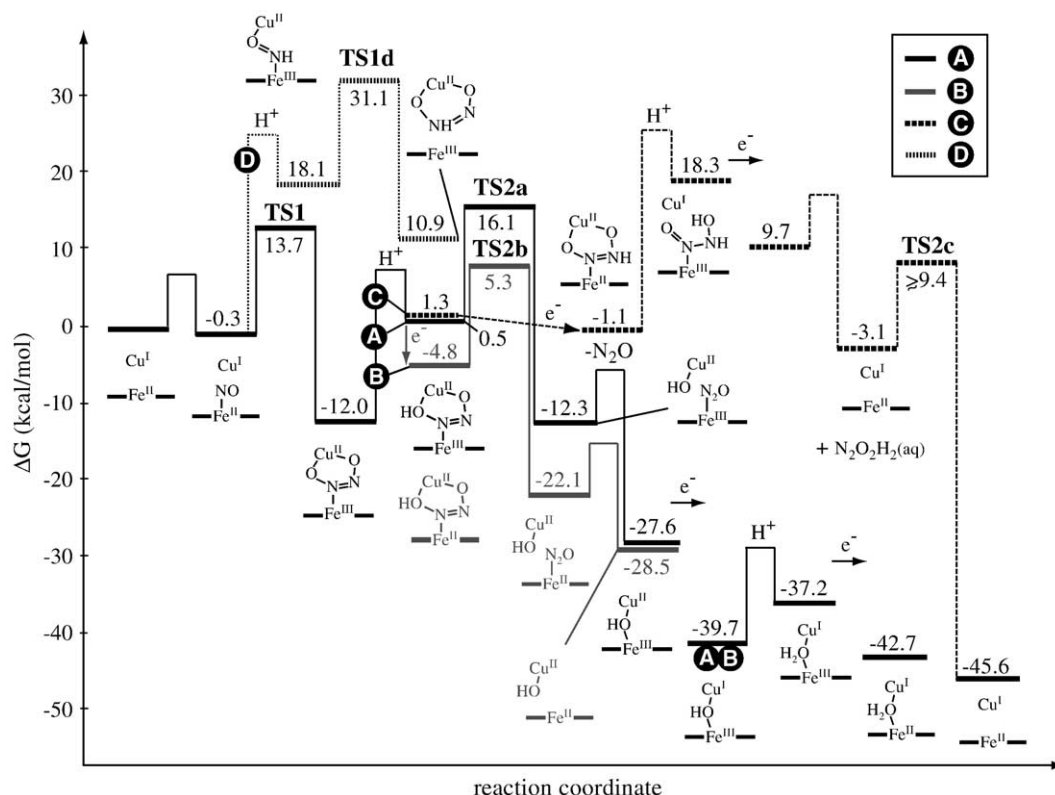


Fig. 14. An overview of the four investigated reaction mechanisms (A–D) for the NO reduction.

the binuclear site. The proton transfer to the five-membered ring (Fig. 5) was estimated to be endergonic by 12.5 kcal/mol. Furthermore, the transfer of an electron to the protonated five-membered intermediate is exergonic by 5.3 kcal/mol. The energetics of the proton and electron transfers are incorporated into the free energy profiles of cases A and B shown in Figs. 10 and 11 and summarized in Fig. 14. The endergonic proton transfer makes the barrier of TS2a 28.1 kcal/mol, which is too high for the reaction to continue. In case B, on the other hand, the endergonic proton transfer is followed by an exergonic electron transfer giving a barrier of TS2b of 17.3 kcal/mol, quite close to the experimental barrier of 19.5 kcal/mol.

Forming the five-membered ring is a quite exergonic process giving a relatively stable intermediate with a backward barrier of around 25 kcal/mol and a forward reaction being the rate limiting step in the catalytic cycle. Thus, the five-membered ring should be experimentally detectable. Furthermore, it should also be possible to isolate this intermediate if one could start the reaction with the enzyme in a mixed valence state, i.e., Cu_A and heme b are oxidized while the binuclear center, heme a_3 and Cu_B , is fully reduced. In this way only the electrons in the binuclear center would be available during the reaction, and according to the results in the present study one more electron is needed to break the N–O bond and form nitrous oxide. The reaction should then stop at the five-membered ring intermediate, and make the latter detectable. The calculated IR frequencies for the N–N vibrational mode of the five-membered ring with different isotopes of NO are given in Table 1. The frequency is shifted by around 42 cm^{-1} by

exchanging ^{14}N for ^{15}N , but hardly affected by the exchange of ^{16}O for ^{18}O .

Except for the quite exergonic process of forming the five-membered ring, most energy is released in the formation of nitrous oxide and the formation of the $\text{Fe(III)}-\text{OH}$ bond while reducing $\text{Cu}_B(\text{II})$.

In cases C and D, both protons and presumably both electrons are transferred before the N–O bond can be broken and N_2O released, the free energy profiles can be seen in Figs. 12 and 13 and the free energy profiles of mechanisms A–D are summarized in Fig. 14. In the five-membered ring the proton affinities of O3 and N2 are very similar, which, as discussed above, implies that both sites should be protonated to the same extent. In case C, a mechanism in which N2 is protonated was investigated. In case D, on the other hand, the nitric oxide coordinating to the reduced binuclear center is first protonated

Table 1
The calculated IR frequencies for the N–N vibrational mode in the hyponitrous acid anhydride intermediate with different isotopes of NO

Calc. ^a	Freq. (cm^{-1})
$^{14}\text{N}^{16}\text{O}$	1305.8
$^{15}\text{N}^{16}\text{O}$	1263.6
$^{14}\text{N}^{18}\text{O}$	1305.6
$^{15}\text{N}^{18}\text{O}$	1263.3

^a The frequencies are scaled by the vibrational frequency scaling factor as determined from data in the CCCBDB (Computational Chemistry Comparison and Benchmark DataBase), which equals 0.962 at the b3lyp/6-31G level of theory.

and then attacked by a second NO leading to a five-membered ring protonated at N1. This intermediate is energetically less favored, since N1 is forced to leave its coordination to the heme iron to become planar. The coordination of N1 to the heme iron is thus the major difference between cases C and D. Both mechanisms are however unfavored compared to case B. The reason for this is the low proton affinity of the coordinated species, leading to endergonic proton transfers. In cases C and D, two proton transfers are needed before the N–O bond can be broken and the energy in the formation of nitrous oxide can be released. The high barriers of the rate limiting steps in cases C and D are thus caused by the high energies of the doubly protonated intermediates.

The conclusion that the most favored mechanism for the reduction of NO in a *ba*₃-oxidase is case B should be reliable since large errors in either the calculations or experiments are needed to favor another mechanism. In case B, both an electron and a proton is transferred to the binuclear site before the N–O bond is broken. This means that the calculated barrier height (TS2b) will only depend on the assumed overall exergonicity of the reaction, and not on the particular cost of the proton and electron transfers. To favor the mechanism in case A compared to case B an error of around 10 kcal/mol in the experimental reduction potentials would be required, making the second electron transfer endergonic by 5.3 kcal/mol, which is very unlikely. The present study clearly favors the mechanism in case B compared to the mechanisms in cases A, C and D.

Appendix A. Supplementary data

Supplementary data associated with this article can be found in the online version at [doi:10.1016/j.bbabbio.2005.11.004](https://doi.org/10.1016/j.bbabbio.2005.11.004).

References

- [1] W.G. Zumft, Nitric oxide reductases of prokaryotes with emphasis on the respiratory, heme-copper oxidase type, *J. Inorg. Biochem.* 99 (2005) 194–215.
- [2] M.R. Cheesman, W.G. Zumft, A.J. Thomson, The mcd and epr of the heme centers of nitric oxide reductase from *Pseudomonas stutzeri*: evidence that the enzyme is structurally related to the heme-copper oxidases, *Biochemistry* 37 (1998) 3994–4000.
- [3] J. Hendriks, A. Warne, U. Gohlke, T. Halita, C. Ludovici, M. Lübken, M. Saraste, The active site of the bacterial nitric oxide reductase is a dinuclear iron center, *Biochemistry* 37 (1998) 13102–13109.
- [4] A. Giuffrè, G. Stubauer, P. Sarti, M. Brunori, W.G. Zumft, G. Buse, T. Soulimane, The heme-copper oxidases of *Thermus thermophilus* catalyze the reduction of nitric oxide: evolutionary implications, *Proc. Natl. Acad. Sci. U. S. A.* 96 (1999) 14718–14723.
- [5] E. Forte, A. Urbani, M. Saraste, P. Sarti, M. Brunori, A. Giuffrè, The cytochrome *cbb*₃ from *Pseudomonas stutzeri* displays nitric oxide reductase activity, *Eur. J. Biochem.* 268 (2001) 6486–6490.
- [6] C.S. Butler, E. Forte, F.M. Scandurra, M. Arese, A. Giuffrè, C. Greenwood, P. Sarti, Cytochrome *bo*₃ from *Escherichia coli*: the binding and turnover of nitric oxide, *Biochem. Biophys. Res. Commun.* 296 (2002) 1272–1278.
- [7] T. Fujiwara, Y. Fukumori, Cytochrome *cb*-type nitric oxide reductase with cytochrome *c* oxidase activity from *Paracoccus denitrificans* atcc 35512, *J. Bacteriol.* 178 (1996) 1866–1871.
- [8] T. Soulimane, G. Buse, G.P. Bourenkov, H.D. Bartunik, R. Huber, M.E. Than, Structure and mechanism of the aberrant *ba*₃-cytochrome *c* oxidase from *Thermus thermophilus*, *EMBO J.* 19 (2000) 1766–1776.
- [9] A.D. Becke, Density-functional thermochemistry: iii. The role of exact exchange, *J. Chem. Phys.* 98 (1993) 5648–5652.
- [10] C. Lee, W. Yang, R.G. Parr, Development of the colle-salvetti correlation-energy formula into a functional of the electron density, *Phys. Rev., B* 37 (1988) 785–789.
- [11] M.J. Frisch, G.W. Trucks, H.B. Schlegel, G.E. Scuseria, M.A. Robb, J.R. Cheeseman, V.G. Zakrzewski, J.A. Montgomery Jr., R.E. Stratmann, J.C. Burant, S. Dapprich, J.M. Millan, A.D. Daniels, K.N. Kudin, M.C. Strain, O. Farkas, J. Tomasi, V. Barone, M. Cossi, R. Cammi, B. Mennucci, C. Pomelli, C. Adamo, S. Clifford, J. Ochterski, G.A. Petersson, P.Y. Ayala, Q. Cui, K. Morokuma, D.K. Malick, A.D. Rabuck, K. Raghavachari, J.B. Foresman, J. Cioslowski, J.V. Ortiz, B.B. Stefanov, G. Liu, A. Liashenko, P. Piskorz, I. Komaromi, R. Gomperts, R.L. Martin, D.J. Fox, T. Keith, M.A. Al-Laham, C.Y. Peng, A. Nanayakkara, C. Gonzalez, M. Challacombe, P.M.W. Gill, B. Johnson, W. Chen, M.W. Wong, J.L. Andres, M. Head-Gordon, E.S. Replogle, J.A. Pople, GAUSSIAN98, Gaussian Inc., Pittsburgh, PA, 1998.
- [12] Schrödinger, Inc., Portland, Oregon, Jaguar 4.2 (2000).
- [13] L.M. Blomberg, M.R.A. Blomberg, P.E.M. Siegbahn, A theoretical study of myoglobin working as a nitric oxide scavenger, *J. Biol. Inorg. Chem.* 9 (2004) 923–935.
- [14] L.M. Blomberg, M.R.A. Blomberg, P.E.M. Siegbahn, W.A. van der Donk, A.-L. Tsai, A quantum chemical study of the synthesis of prostaglandin g₂ by the cyclooxygenase active site in prostaglandin endoperoxide synthase 1, *J. Phys. Chem., B* 107 (2003) 3297–3308.
- [15] D.J. Tannor, B. Marten, R. Murphy, R.A. Friesner, D. Sitkoff, A. Nicholls, M. Ringnalda, W.A. Goddard III, B. Honig, Accurate first principles calculation of molecular charge distributions and solvation energies from ab initio quantum mechanics and continuum dielectric theory, *J. Am. Chem. Soc.* 116 (1994) 11875–11882.
- [16] M.R.A. Blomberg, P.E.M. Siegbahn, G.T. Babcock, Modeling electron transfer in biochemistry: a quantum chemical study of charge separation in *Rhodobacter sphaeroides* and photosystem ii, *J. Am. Chem. Soc.* 120 (1998) 8812–8824.
- [17] D.M. Popović, J. Quenneville, A.A. Stuchebrukhov, Dft/electrostatic calculations of pK_a values in cytochrome *c* oxidase, *J. Phys. Chem., B* 109 (2005) 3616–3626.
- [18] L.A. Curtiss, K. Raghavachari, R.C. Redfern, J.A. Pople, Assessment of gaussian-3 and density functional theories for a larger experimental test set, *J. Chem. Phys.* 112 (2000) 7374–7383.
- [19] P.E.M. Siegbahn, M.R.A. Blomberg, Density functional theory of biologically relevant metal centers, *Annu. Rev. Phys. Chem.* 50 (1999) 221–249.
- [20] P.E.M. Siegbahn, M.R.A. Blomberg, Transition-metal systems in biochemistry studied by high-accuracy quantum chemical methods, *Chem. Rev.* 100 (2000) 421–437.
- [21] M.R.A. Blomberg, P.E.M. Siegbahn, A quantum chemical approach to the study of reaction mechanisms of redox-active metalloenzymes, *J. Phys. Chem., B* 105 (2001) 9375–9386.
- [22] C.E. Cooper, Nitric oxide and iron proteins, *Biochim. Biophys. Acta* 1411 (1999) 290–309.
- [23] M.H. Vos, G. Lipowski, J.-C. Lambry, J.-L. Martin, U. Liebl, Dynamics of nitric oxide in the active site of reduced cytochrome *c* oxidase *aa*₃, *Biochemistry* 40 (2001) 7806–7811.
- [24] L.M. Blomberg, M.R.A. Blomberg, P.E.M. Siegbahn, A theoretical study on the binding of o₂, no and co to heme proteins, *J. Inorg. Biochem.* 99 (2005) 949–958.
- [25] V. Shafirovich, S.V. Lymar, Nitroxyl and its anion in aqueous solutions: spin states, protic equilibria, and reactivities toward oxygen and nitric oxide, *Proc. Natl. Acad. Sci. U. S. A.* 99 (2002) 7340–7345.
- [26] P. Hellwig, T. Soulimane, G. Buse, W. Mantele, Electrochemical, ftr, and uv/vis spectroscopic properties of the *ba*₃ oxidase from *Thermus thermophilus*, *Biochemistry* 38 (1999) 9648–9658.
- [27] P. Moënne-Loccoz, O.-M.H. Richter, H.-W. Huang, I.M. Wasser, R.A. Ghiladi, K.D. Karlin, S. de Vries, Nitric oxide reductase from

- Paracoccus denitrificans* contains an oxo-bridged heme/non-heme diiron center, *J. Am. Chem. Soc.* 122 (2000) 9344–9345.
- [28] P.E.M. Siegbahn, M.R.A. Blomberg, L.M. Blomberg, Theoretical study of the energetics of proton pumping and oxygen reduction in cytochrome oxidase, *J. Phys. Chem., B* 107 (2003) 10946–10955.
- [29] A. Daiber, H. Shoun, V. Ullrich, Nitric oxide reductase (p450_{nor}) from *Fusarium oxysporum*, *J. Inorg. Biochem.* 99 (2005) 185–193.
- [30] M.A. Vincent, I.H. Hillier, J. Ge, How is n–n bond formation facilitated by p450 reductase? A DFT study, *Chem. Phys. Lett.* 407 (2005) 333–336.